Extended Multi-Plane Pressure Mode Matching for CFD/CAA Coupling

Christian Weckmüller, Attila Fritzsch, Sébastien Guérin
German Aerospace Center, Institute of Propulsion Technology, Engine Acoustics Dept., Berlin
Email: christian.weckmueller@dlr.de

Introduction

Hybrid CFD/CAA approaches allow a drastic reduction of the computational ressources required for the prediction of turbomachinery noise. The generation and propagation of BPF tones in bypass ducts is a possible application of hybrid approaches. The method works as follows. Inside the region surrounding the rotor/stator stage (source region), the unsteady Reynolds Averaged Navier-Stokes equations are solved. Outside of this domain, the sound propagation is simulated with the Euler equations. At the CFD/CAA interface, only the acoustic fluctuations are transfered into the CAA domain to avoid the occurence of instabilities during the CAA simulation.

Two coupling strategies are known by the authors. The first technique is based on a Helmholtz decomposition of the velocity field [1]. In this method, the acoustic and vorticity perturbations are splitted locally, which should enable the treatment of complex flow configurations. Unfortunately, this method is suitable only for incompressible turbulent flows. The second technique, so-called tripple plane pressure mode matching method (TPP), was introduced by Ovenden and Rienstra [2]. This method has the advantage to be applicable to compressible turbulent flows. A prerequisite is to know the analytical solution describing the sound propagation according to the geometry and background mean flow.

The objective of this paper is to extend the TPP method to improve the acoustic splitting. Indeed, the original TPP method does not provide accurate results when the level of the aerodynamic perturbations is too high compared to that of the acoustic perturbations. This can be the case close to the stator (see Fig. 1). Thus, to apply the TPP method with confidence, the CFD simulations must be able to propagate the acoustic perturbations over an axial distance of several chord lengths downstream of the stator, which increases the computational costs. By incorporating an aerodynamic model, the physical description of the fluctuating pressure field is improved, which improves the quality of the modal decomposition for a given ratio of aerodynamic to acoustic perturbations. Thus, it is possible to reduce the distance between the source region and the planes where the pressure is modal decomposed. In the present paper, the extended pressure mode matching method is applied to CFD data of the DLR UHBR Fan [3].

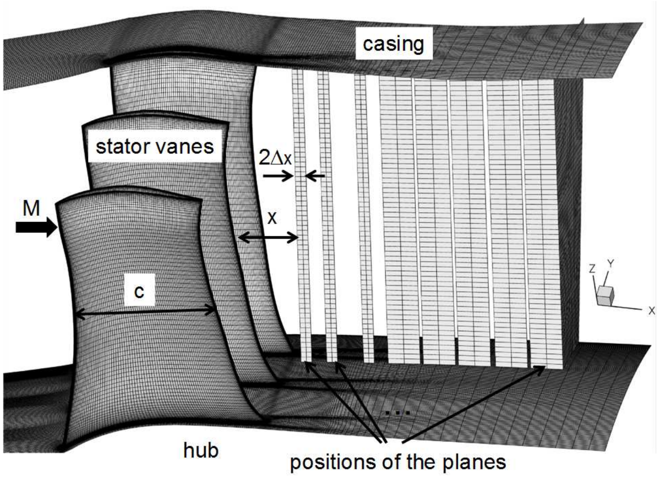

Figure 1: Projection of the CFD mesh on the stator vanes and duct walls. Also shown is the position of the planes where the modal decomposition is applied.

Extension of the splitting method

The tripple plane pressure mode matching method (TPP) was proposed by Ovenden and Rienstra [2]. It bases upon an asymptotic formulation of the sound propagation in slowly varying ducts [4]. Thus the 1D isentropic background mean flow and the transversal and axial wave numbers can vary slowly along the duct. A linear system of equations is solved

$$(\mathcal{M}^2 + \mathcal{N}^2 + \mathcal{Q}^2)a = \mathcal{M}p_0 + \mathcal{N}p_1 + \mathcal{Q}p_2 \qquad (1)$$

in which the vector a denotes the pressure modal amplitude of the acoustic modes and the vectors p_i the CFD pressure measured at the three axial planes. The entries of the matrices $\mathcal{M}, \mathcal{N}, \mathcal{Q}$ depend on the modal basis. In case of orthogonality of the modal basis, the matrices will show a band structure. Therefore, only the amplitudes of the downstream and upstream propagating (m, n)-modes are related. The problem is perfectly matched when no aerodynamic perturbations are present in the CFD data. Otherwise, the aerodynamic perturbations are projected onto the right-hand side vectors p_i of the linear system and will add some errors to the amplitudes.

In the case of plane waves, De Roeck [1] suggested to add an aerodynamic model to the modal basis. The key idea is that vorticity waves are convected with the mean flow velocity. While the axial wave numbers $k_{x,mn}$ of the acoustic modes are related to their transversal wave numbers $k_{r,mn}$ by the dispersion relation, the axial wave numbers of the aerodynamic perturbations are independent of the mode order. The TPP method is extended by adding a model applying this principle. The aerodynamic model uses the same eigenfunctions to describe the cirfumferential and radial shape of the modes, but uses different axial wave numbers. Instead of the acoustic wave number $k^{\pm}_{x,mn}$, an aerodynamic wave number

$$k_{ae} = \frac{k}{M_x}, \tag{2}$$

is introduced. In Eq.(2), k is the free-field wave number and M_x the cross-sectional averaged axial Mach number of the mean flow. The value of k_{ae} changes slowly in the axial direction following the variations of the duct contour. This model describes the convection of perturbations with the mean flow, but does not account for the effects due to the wake expansion, neither the viscous dissipation. The error due to these simplifications should be negligible if the evaluation planes are closely spaced, as it is the case in our applications. While it is meaningful to speak of acoustic (m, n)-modes, because the space-time structure of those modes propagates without changing along the duct, this is not the case for the aerodynamic modes. Therefore, no physical interpretation will be given to them: the aerodynamic modes just help to improve the splitting and reconstruct the aerodynamic pressure field.

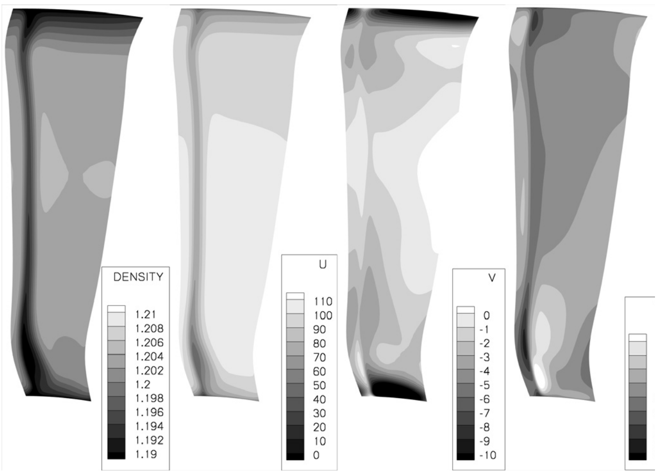

Figure 2: Density and velocity (r, θ)-slices of the mean flow field behind one stator segment ($x/c = 0.32$).

Numerical simulations

The unsteady flow field of the DLR UHBR fan [5] is calculated in approach condition (3187 rpm, mass flow 47.3 kg/s, PR=1.06) using the DLR CFD solver TRACE (Turbomachinery Research Aerodynamic Computational Environment [6]) developed by the Department of Numerical Methods of the Institute of Propulsion Technology. The fan is composed of 22 rotor blades and 38 stator vanes. The phase-lagged method [7, 8] enables to reduce the computed problem to one segment for the rotor and another one for the stator. A multi-block structured grid of 3.3 millions nodes is used. The time integration is realized with 256 time steps per blade passing, and 20

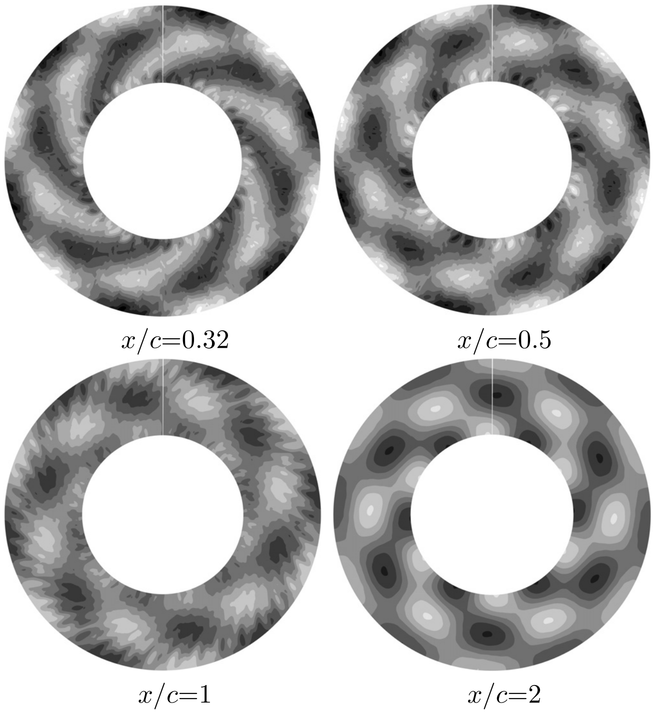

Figure 3: Instanteneous BPF2 pressure field at 4 different axial positions behind the stator.

sub-iterations in the dual-time stepping algorithm. More details are given in Ref. [3]. In Fig. 2, a slice of the steady flow downstream of the stator segment is shown. Notice that there is almost no swirl and that the boundary layer is about 12% of the duct height.

Results

The extended multi-plane pressure mode matching method (XTPP) is applied at 8 different positions between x/c =0.32 and 2 (see tab. 1). Here, the distance x denotes the spacing between the stator trailing edge at midspan and the centre plane, and c the chord length at midspan. Each analysis is performed with three planes separated by a constant spacing specified in Tab. 1. With the DLR UHBR fan the blade passing frequency is cut-off at approach condition. In the simulations, the BPF2 appears to be the strongest harmonic component. According to the Tyler-Sofrin's rule [9], the rotor-stator interaction modes of azimuthal order $m = ..., -44, -6, 32, ...$ should be present at the BPF2 frequency[1]. The following definition of the cut-on factor, strictly valid for a uniform flow in a duct of constant cross section,

$$\alpha_{mn} = \sqrt{1 - (1 - M_x^2)\frac{\sigma_{mn}^2}{(kR)^2}}, \tag{3}$$

is used to separate cut-on and cut-off acoustic modes. In that equation, σ_{mn} is the eigenvalue related to the radial mode shape function. According to that definition, only the modes (m, n)=(-6,0), (-6,1), (-6,2), and (-6,3) are cut-

[1]In this paper, positive m denote modes rotating in the positive θ-direction of an orthogonal positive defined system of coordinates, whose x-axis is pointed in the direction of the mean flow.

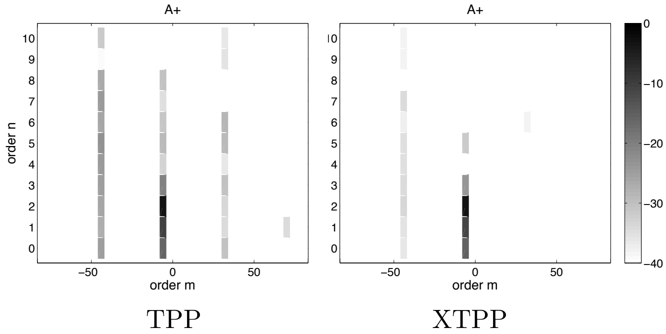

Figure 4: Pressure modal amplitudes of the downstream propagating waves (BPF2, $x/c = 1$).

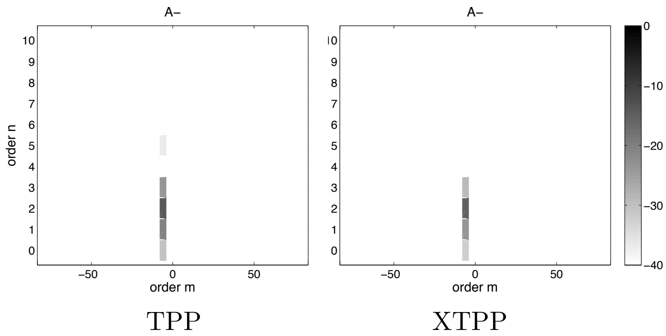

Figure 5: Pressure modal amplitudes of the upstream propagating waves (BPF2, $x/c = 1$).

on for the BPF2. The modal decomposition presented below was done with all modes such as $-81 \leq m \leq 81$ and $0 \leq n \leq 10$.

In Fig. 3, the CFD pressure data of BPF2 extracted at 4 axial positions are shown. A dominant pattern with $|m| = 6$ can be identifed. With increasing distance to the vanes, the high-order perturbations tend to vanish. At $x/c = 2$, the pressure field is dominated by a limited number of acoustic modes. The dissipation of the high-order perturbations could be due either to some physical effects modelled by the RANS equations, or some numerical dissipation resulting from the grid coarsening.

The levels A_{mn} of the modal decomposition performed at $x/c = 1$ are shown in details in Fig. 4, 5 and 6. As expected, only the Tyler and Sofrin's modes are found. More important is to notice that the high-order modes $m = -44$ are interpreted as being cut-off in the orginal TPP method while an aerodynamic nature is attributed to them by the XTPP method. This second interpretation is more likely since the distance to the stator is high for those cut-off modes whose amplitude decreases exponentially. The two techniques predict about the same amplitude for the cut-on modes as it will be shown hereafter. One can also observe that the amplitudes of the A^+ modes decreases at the benefit of the A^{ae} modes. As stated by Ovenden [2] in the case of an orthogonal modal basis the linear system in Eq.(1) relates only the amplitudes of the downstream and the upstream propagating acoustic waves of the same order (m, n). In the new model, the amplitudes

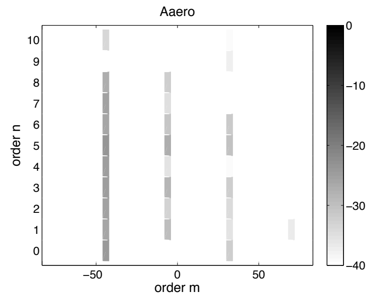

Figure 6: Pressure modal amplitudes of the aerodynamic perturbations in XTPP (BPF2, $x/c = 1$).

of the acoustic waves are also connected to the convected waves by a single equation. Even though the level is much smaller, some energy is still attributed to the cut-off modes within the XTPP method. This may have several reasons: i) the aerodynamic model describes a mean axial convection without radial and circumferential components, ii) the aerodynamic model does not account for any dissipation, and iii) the acoustic model for slowly varying ducts applied here does not account for neither the variations of the radial flow profile nor the presence of a swirl. In Fig. 7, the acoustic and aerodynamic parts are represented separately.

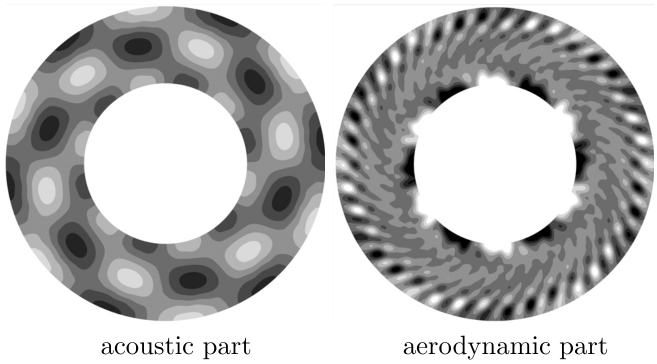

Figure 7: Pressure field reconstruction at $x/c = 1$. The scaling of the aerodynamic perturbations is changed to emphasise the structure.

Figures 8 and 9 compare the acoustic power for the four cut-on modes of BPF2, obtained with the TPP and XTPP methods. The following definition of the acoustic power is used:

$$P^{\pm}_{mn} = \pm\pi R^2 \frac{\alpha_{mn}(1 - M_x^2)^2}{\rho_0 c_0 (1 \mp \alpha_{mn} M_x)^2} |A^{\pm}_{mn}|^2. \qquad (4)$$

The (positive) downstream propagating modes are directly produced at the stator. The amplitude of the radial components n =0,1 and 2 vary by 10 dB with TPP and only by 2 dB with XTPP. The waves propagating in the negative (upstream) direction are due to numerical reflections at the outlet. Their variations of amplitude are larger but still remain lower with the XTPP method. The reason why the amplitude of the mode (-6,3) decreases along the duct is not understood yet.

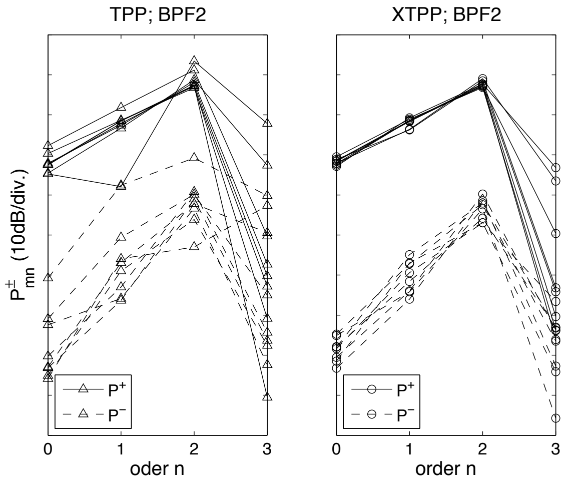

Figure 8: Power amplitude of the Tyler and Sofrin modes of azimuthal order $m = -6$: (left) original TPP, and (right) version extended to aerodyanmic modes. The results of eight investigated axial positions are overlayed to evidence the improvement using XTPP.

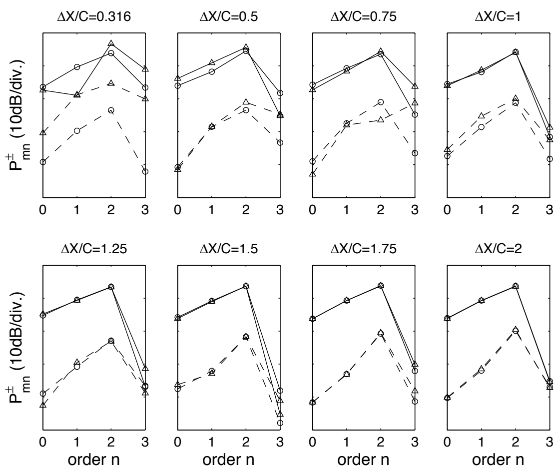

Figure 9: Same results as in Fig. 8 showing that TPP and XTPP give the same solution only at high distance to the vanes.

Conclusion

The tripple plane pressure mode matching method introduced by Ovenden and Rienstra [2] was extended by introducing a new modal basis which takes into account the aerodynamic pressure fluctuations produced by the rotor and stator wakes. In the presented study, the same eigenfunctions for acoustics and aerodynamics are used. With TPP, the modal decomposition of the URANS simulation is improved. The new XTPP not only increases the quality of the splitting close to the stator but also enhances our understanding of the physical mechanisms. Thus pressure disturbances associated to the cut-off acoustic modes are separated from those due to the aerodynamic perturbations. It can be speculated that further improvements could be obtained by chosing a set of acoustic and aerodynamic eigenfunctions more adapted to the flow.

References

[1] W. De Roeck, G. Rubio, and W. Desmet. On the Use of Filtering Techniques for Hybrid Methods in Computational Aero-Acoustics. In *Proceedings of the International Conference on Sound and Vibration, ISMA 2006*, Leuven, Belgium, 2006.

[2] N.C. Ovenden and S.W. Rienstra. Mode-Matching Strategies in Slowly Varying Engine Ducts. *AIAA Journal*, 42:1832–1840, September 2004.

[3] C. Weckmüller, S. Guérin, and G. Ashcroft. CFD/CAA Coupling Applied to DLR UHBR-Fan: Comparison to Experimantal Data. In *Proceedings of the 15th AIAA/CEAS-Aeroacoustics Conference*, Miami, Florida, May 11-13 2009. AIAA-paper 2009-3342.

[4] S.W. Rienstra. Sound Transmission in Slowly Varying Circular and Annular Lined Ducts with Flow. *Journal of Fluid Mechanics*, 380:279–296, 1999.

[5] B. Kaplan, E. Nicke, and C. Voss. Design of a highly efficient low-noise Fan for Ultra-High Bypass Engines. In *Proceedings of ASME Turbo Expo 2006*, Barcelona, Spain, May 8-11 2006. 2006-GT-90363.

[6] D. Nuernberger, F. Eulitz, S. Schmitt, and A. Zachcial. Recent Progress in the Numerical Simulation of Unsteady Viscous Multistage Turbomachinery Flows. In *Proceedings of the 15th International Symposium on Air Breathing Engines*, 2001. ISABE-2001-1081.

[7] G.A. Gerolymos, G.J. Michon, and J. Neubauer. Analysis and Application of Chorochronic Periodicity in Turbomachinery Rotor/Stator Interaction Computations. *Journal of Propulsion and Power*, 18:1139–1152, 2002.

[8] R. Schnell. Investigation of the Acoustic Nearfield of a Transonic-Fanstage by Time-Domain CFD-Calculations with Arbitrary Blade Counts. In *ASME Turbo-Expo 2004, 7.-14. Juni 2004, Wien/Österreich*, Wien, Österreich, June 7-14 2004. 2004-GT-54216.

[9] J.M. Tyler and T.G. Sofrin. Axial flow compressor noise studies. *SAE Transactions*, 70:309–332, 1962.

Plane	Parameters			
	x/c	M_x	R	$\Delta x/\lambda$
1	0.32	0.288	0.420	0.07
2	0.50	0.286	0.422	0.07
3	0.75	0.283	0.424	0.07
4	1.00	0.281	0.427	0.21
5	1.25	0.278	0.430	0.21
6	1.50	0.274	0.432	0.21
7	1.75	0.270	0.436	0.21
8	2.00	0.266	0.439	0.21

Table 1: Axial position of the centre planes, axial Mach number, duct radius, axial spacing between the 3 planes.